https://doi.org/10.1016/j.mtener.2019.04.006

Highly active electron-affinity for ultra-low barrier for alkaline ORR in Pd_3Cu

Tong Wu, Mingzi Sun and Bolong Huang*

Department of Applied Biology and Chemical Technology, The Hong Kong Polytechnic University, Hong Hum, Kowloon, Hong Kong SAR, China.

*Email: bhuang@polyu.edu.hk

Abstract

The call for clean and sustainable energy raises tremendous research interests in fuel cell. However, the efficiency of low-temperature fuel cell is heavily impeded by the sluggish cathode reaction, the oxygen reduction reaction (ORR), even with the state-of-the-art Pt catalyst. Advanced ORR catalysts with better activity and lower expense are of great research interest for the development of clean energy. Pd_3Cu alloy is one of the potential non-Pt based ORR catalysts owing to its excellent balance between activity, long term stability and cost. Alkaline ORR so far receives much less theoretical study interest although alkaline medium is found to be beneficial to ORR in many aspects. Aimed to gain more theoretical insight into the reactivity of Pd_3Cu and mechanistic information of alkaline ORR, mechanism study was conducted by applying DFT calculations. The electron-affinitive of Pd_3Cu has been activated by the *d-d* coupling between Pd and Cu. Adsorption strengths of ORR intermediates, and especially their preferences to various adsorption sites were carefully examined and discussed. The adsorption analysis prompted us a possible ORR mechanism on Pd_3Cu surface. Reaction pathway calculations based on this mechanism unveiled an energetically favorable reaction path with an ultra-low overpotential. This theoretical support supplied a new direction for the reactivity of catalyst.

As the increasing demand for greener energy supplies, tremendous interest has arisen for environmentally friendly fuel cells, especially about the key reaction on cathode, oxygen reduction reaction (ORR)[1-6]. Beyond the commonly studies alloys materials, some graphene/metal composite materials are emerging as promising ORR catalysts as well [7-10]. Compared with the acidic condition, the alkaline condition offers several advantages for ORR including faster kinetics, optimized adsorption strengths[11], the thermodynamic preference on pathway[12], wider selections of material[8] and less corrosive conditions for materials. Presently, the research of alkaline ORR is usually characterized by mass activity and the current density. The more complex alkaline ORR has largely constrained the theoretical research in recent years. Pd has been found as a promising candidate that shows better performance in alkaline fuel cells with ethanol and propanol[13]. The lower ORR activity than Pt has been ascribed to the overbinding effect of oxygen on the Pd surface[14]. By introducing Pt or other transition metals (e.g., Co, Fe, Cu, Ni, Au etc.) to form alloys, the ORR activity of Pd can be largely improved, and the ORR activity of Pd-M alloys can exceed those of Pt[13]. Cu is a good candidate but has rarely been discussed before. Owing to its positive electrochemical potential in the solution, high stability can be expected. Both crystal structure and electronic structure modification by the incorporation with Cu can be achieved[15]. The durability of the catalyst is also an important factor controlling the practical performance of catalysts. The Pd_3Cu has a significantly smaller loss of Cu than PdCu after extensive cycles[16]. Besides, previous works also suggested that the Pd_3Cu exhibited significant resistance to OH^- poisoning, allowing the continual O_2 adsorption on active sites for longer durability[17-19]. Thus, an in-depth theoretical study is necessary on the Pd_3Cu for further understanding of ORR activity under alkaline conditions. In this work, DFT calculations were applied to investigate the alkaline ORR process involved with the detailed binding strength of different sites as the selectivity preference. Related calculation setup can be found in the ***Supporting Information***. We have explored a new possible direction for theoretical ORR study in the alkaline environment, which can serve as a support to the d-band center theory for widening ORR activity studies and applications.

As O_2 adsorption is the prerequisite of an efficient ORR on the surface, the strength of it determines whether the reaction is easy to initiate. Based on the accurate orbital energy calculations, our previous works have successfully identified the activation of electronegativity of Pd and transition metals via the orbital coupling[20-21]. Especially, the d-d orbital coupling will largely enhance the orbital energy that further boost the electron transfer for efficient electrocatalysis[20]. As for Pd with a $4d^{10}$ electron configuration, the relatively inert reactivity can be activated to electron-affinity through the introduction of Cu (**Figure 1**). Through the strong d-d coupling between Pd and Cu, the extra active electrons from Cu [$3d^{10}4s^1$] contribute to the formation of an electron-affinitive $4d^{10+\delta}$ Pd, which can break the constrains of electron supply to achieve the firm adsorption of O_2 to form stable adsorbed O_2^{2-}. Following the previously reported approach in calculating the orbital energy, we confirmed that the Pd shows a stronger electron-affinity with a larger δ value, supporting the higher activity in electron transfer. It has also been reported that a stronger oxygen adsorption strength brings a higher initial current density in cell operation for a better cell performance[22]. Thus, the O_2 adsorption energy rather than the O adsorption energy has been considered in this study. The d-band-center calculations and the average O_2 adsorption energies of three surfaces have been summarized in **Table S1 and Figure S1**. The calculation of d-band center and the average adsorption energies is consistent with the d-band center theory that the position of d-band center is proportional to the adsorption strengths of the adsorbates[23]. However, a deeper look into the specific adsorption strengths on available sites reveals different results, in which the

fcc site on the (111) surface has the overall strongest O_2 adsorption strength among the sites on three surfaces. This unique O_2 adsorption strength comparison reminds us that the general ORR adsorption study method has neglected the active site preference on the surface, which might play a crucial role.

Another highlight is the detailed comparison of O_2 adsorption preferences on the active sites of the three surfaces (**Figure 2a-2c**). O_2 has a significant adsorption preference on the (111) surface, while it does not show the same extent of site preference on the (100) and (110) surfaces. The O=O bond length has remained similar on the (111) and (110) surfaces, while the hollow site of the (100) surface has experienced an evident increase after adsorption. The *fcc* sites on (111) adsorbs O_2 remarkably stronger than other sites on the (111) surface, with energy differences varying from 1.59 eV to almost 3 eV. Although the O_2 adsorption strength on the (100) hollow site is approximately as strong as that on (111) *fcc*, the hollow site is just slightly stronger than the bridge site with less than 0.5 eV in energy difference. For the (110) surface, no significant energy difference like that of the (111) surface could be observed. The unexpected strong adsorption strength of *fcc* and the significant adsorption preference on (111) has raised our interest. In comparison, the H_2O adsorption energies on the (111) surface vary in a small range within 0.539 eV (**Table S2 and Figure 2d**). This is distinct from the O_2 adsorption on the (111) surface that the largest energy difference is up to ~3 eV. The small energy difference indicates that H_2O hardly shows a specific preference toward the active sites on (111), indicating an easy migration on the (111) surface. The H_2O will not hinder the O_2 adsorption on the active sites since the adsorption energies of H_2O are much weaker than that of O_2. If the favourable adsorption sites for other ORR reactants are different from O_2, it is possible to resolve the obstacle in ORR catalysis that the active sites of O_2 are blocked by other adsorbates. Moreover, it opens the possibility for the separate tuning of adsorption strengths for different adsorbates on the surface. Therefore, the (111) surface will be our research focus. Previously, researchers focused on adjusting the O adsorption energy of the surface model to obtain a better ORR activity than Pt[24-31]. This idea is originated from the ORR volcano plot proposed by Nørskov et al. and the internal scaling law that the binding energies of ORR intermediates are correlated with each other[13]. However, this correlation of O and other intermediates has been proven to be applicable only on pure transition metal surfaces, in which only strain effect is in control of the d-band centre values [30].

For the alloy surface in which both ligand and strain effects are presented, the O binding energy does not correlate with the binding energies of O_2, OOH and OH well. The projected density of states (PDOS) of O_2 on surfaces has confirmed a similar overlap with the surface on most active sites, in which the over-binding on Pd sites can be observed. This can be attributed to most of the adsorption of O_2 preferred the *fcc* sites after relaxation except for the strong binding with the surface of Pd. The O_2 energy also has a much better correlation with the binding energies of OOH and OH due to the similarities in their PDOS(**Figure S3-S4**). The OH adsorption energy can affect the energy barrier of the electron/proton transfer step and the removal of the products in alkaline ORR. As O_2 adsorption energy has better correlation with OH, it serves as a better ORR activity parameter than O adsorption energy.

The extraordinary O_2 adsorption selectivity preference on the (111) surface suggests that simply treating the surface as a whole in calculations could lead to inaccurate estimations of the surface reactivity. Although the average adsorption energies of the active sites show good correlation with

the surface d-band centre position, the strongest adsorption of O_2 on the *fcc* site of the (111) surface does not concur with d-band theory conclusion that the (111) should have the weakest average adsorption strength. Therefore, investigation of the adsorption preference on the surface can provide supporting information on the surface reactivity of the surface and enhance the application of d-band centre theory. Moreover, analysing the adsorption preferences of ORR adsorbates sheds light on the separate tuning of ORR adsorbates adsorption strengths. Comparison of adsorption strengths of O_2 and OH^- shows that the O_2 adsorbs ~0.2 eV stronger on *fcc* while OH-species are more stable on *hcp* and bridge sites (**Figure S2a**), indicating that the OH poisoning by blocking the *fcc* sites for O_2 is less likely to occur on the surface. If the surface sites can be tuned to further weaken the OH^- adsorption while maintaining strong adsorption of O_2, the ORR activity could be further improved. The adsorption preference of $4OH^-$ on the active adsorption sites on (111) are also important (**Table S3**). The OH^- adsorption strengths on Pd and Cu sites are relatively weak among the active sites. The *fcc* site ranks third in adsorption energy, while the *hcp* and bridge sites are approximately 0.5 eV stronger and in a similar energy level. These results indicate that the hydroxide is relatively unstable on Pd, Cu and *fcc* active sites. Based on this, the chemisorption energy of OH^- are also considered on the Pd_3Cu (111) *fcc* site (**Table S4**). The chemisorption of OH^- is thermodynamically favourable with an energy of -3.700 eV, which can promote the reduction of adsorbed O* to the adsorbed OH*.

Our work emphasis the investigation of ORR intermediates adsorption preferences towards the active sites on surface. Here we proposed the associated mechanism of alkaline ORR as follows:

$$O_2 + * = O* \quad (1)$$
$$O_2* + 2H_2O + 2e = O_2^{2-} + 2H_2O \quad (2)$$
$$O_2^{2-} + 2H2O = OOH^- + OH^- + H_2O \quad (3)$$
$$OOH^- + OH^- + H_2O = O* + 2OH- + H_2O \quad (4)$$
$$O* + 2OH^- + H_2O = OH* + 3OH^- \quad (5)$$
$$OH* + 3OH^- = 4OH^- \quad (6)$$

The adsorption energies of two important ORR intermediates, OOH^- and O* were calculated. $*OOH^-$ is the characteristic intermediate generated from the associative mechanism meanwhile O* will dominate the dissociative mechanism. As OOH^- and O* both originate from the adsorbed O_2, their adsorption calculations were also applied on the *fcc* site of Pd_3Cu (111) due to the preference of O_2. The optimized configurations and adsorption energies of alkaline ORR species on active sites of Pd_3Cu (111) are shown in **Figure S2 and Table S5**. The adsorption energies difference among O_2, OOH^- and O* will unravel a possible dominant reaction path of alkaline ORR on Pd_3Cu (111). OOH^- has more stable adsorption on the surface than O* and O_2. O* is 1 eV weaker than O_2 and nearly 2 eV weaker than $*OOH^-$. Judging from their energy differences with the O_2 adsorption energy, formation of $*OOH^-$ will be easier, which is aligned with our proposed associative mechanism.

Based on our proposed mechanism, the optimized structure configurations and corresponding reaction energy path have been displayed in **Figure 3 and Table S6**. All energies have considered the change of entropy and zero-point energy. In accordance with the adsorption behaviour of O_2, the first reaction step of O_2 adsorption will also occupy the *fcc* site. The black line in **Figure 3b** is the reaction energy change at U=0 V that represents the energy level when the cell is short-circuited.

From this direct and comprehensive method, it can be seen that all of the steps are exothermic. The bias effect of the applied potential was then considered by shifting the energy of all electron involved states by -neU (n is the number of electrons). Since we cannot mechanically apply the method of acidic situation with U= 1.23 V in the alkaline medium, we have set the equilibrium potential of ORR in pH=14 at U= 0.828 V. At this potential, the only endothermic step is the final reduction of the OH* to OH^- with the energy barrier of 0.590 eV. Following the estimation method proposed by Nørskov et al.[13], the overpotential is estimated to be η=0.590 V to overcome this largest energy barrier. Therefore, at potentials lower than $U=U_0-\eta$ =0.828 V-0.590 V= 0.238 V (green line in **Figure 3b**), all the steps become exothermic. Moreover, the final desorption step of OH^- to the solution only shows the energy of -0.590 eV at U=0 V, suggesting that the binding strength of OH^- to the surface is easy to overcome. In other words, when the adsorbed OH* is reduced, it would prefer to be released to the aqueous phase, which means the chance of surface poisoning by the $4OH^-$ is low. With these results, we can preliminary conclude that the alkaline ORR on the Pd_3Cu (111) will be initiated by firm adsorption of O_2 and facilitated by the easy removal of the final product OH^-. This difference in adsorption preference suggests this surface is theoretically promising in alkaline ORR catalysis. It is worth saying that such a method of overpotential estimation is derived from the acidic ORR. The present challenges for alkaline ORR originated from the complexity of alkaline ORR and the difficulty of estimating the standard potential of ORR in alkaline conditions. It has been shown that the effect of pH to OH^- adsorption strength is very complex, involving the co-adsorption effect of hydrogen and even alkali cation, and it has a significant impact on the electrocatalytic properties of the electrode surface. More accurate evaluation of the hydroxide adsorption in alkaline medium requires a much more complicated surface modelling than that of an acidic medium[30,31]. Thus, the interpretation of calculation results of alkaline ORR has not reached a consensus yet. Our method has been derived from the widely-accepted method of acidic ORR with the modification based on alkaline conditions, which has offered a clear and direct understanding of the mechanism.

In conclusion, our work has supplied a new approach to predict the predominant ORR mechanism on the surface through the adsorption preference and electron electron-affinity (**Table 1**). The detailed analysis of surface adsorption preference offers novel insights into the complex alkaline ORR process on the alloy surface. The DFT calculations have revealed the electronic reactivity as well as adsorption of intermediates on Pd_3Cu surfaces in alkaline ORR. The unique O_2 adsorption behaviours on the *fcc* site of (111) surfaces have been observed and lead to the in-depth analysis of the associative reaction mechanism concerning the adsorption strength of intermediates. The overall energetically favorable reaction trend with ultra-low overpotential has been discovered on the electron-affinitive Pd3Cu as a potential catalyst for alkaline ORR. Our work has strengthened the wider application of d-band-centre theory achieving efficient ORR in the alkaline environment for future applications in fuel cells.

The author BH gratefully acknowledges the support of the NSFC (21771156) and the ECS fund (PolyU 253026/16P) from the RGC in HK.

Conflicts of interest

There are no conflicts to declare.

Table 1. Brief summary of conclusions

Summary of Conclusions		
Highlight of study		**Details**
Electron affinity activation by alloying Cu		Activating the inert Pd $4d^{10}$ shell for stronger electron transfer to O_2
Adsorption site study	**d-band center**	(100) > (110) > (111)
	Overall E_{ads} for O_2	• (100) > (110) > (111) • Follows d-band center model
	Strongest adsorption site for O_2	• ***fcc* on (111)** • **Would be overlooked if purely consider d-band center and overall E_{ads}**
	O_2 adsorption site bias	**Only on (111)**
	Inspiration	Adsorption study should be **specific to the available sites** of surface
Thermodynamics of ORR on Pd_3Cu (111)		1. Only one endothermic step at equilibrium potential 2. Ultra-low overpotential: $\eta = 0.238$ V 3. Potential efficient alkaline ORR catalyst

Figure 1.

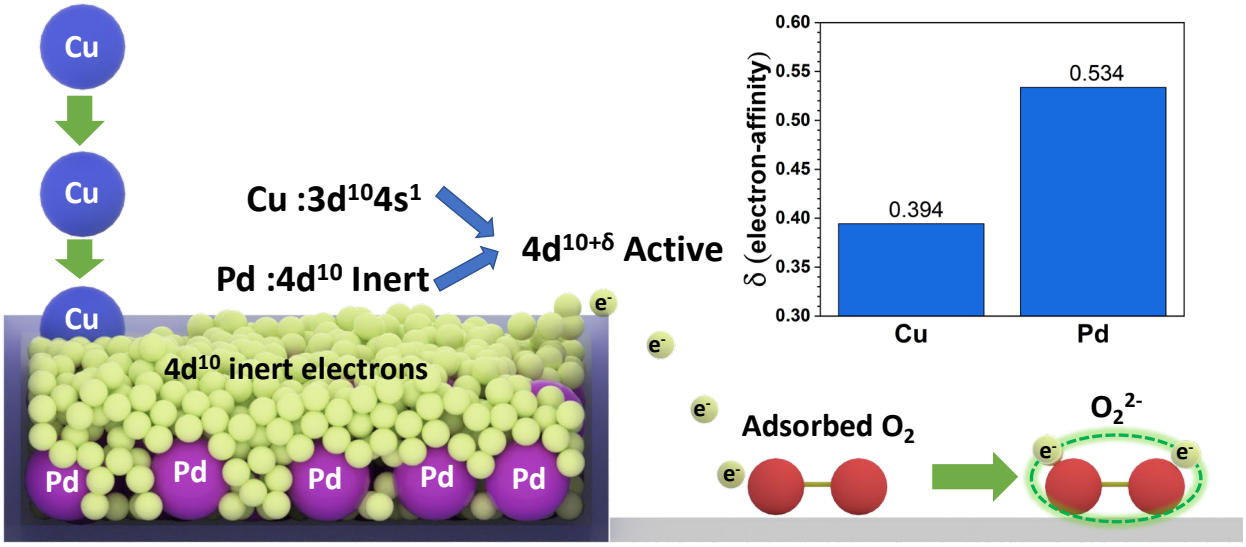

Figure 1 | Illustration of the active electron-affinity of Pd_3Cu for boosting the alkaline ORR. Inset: Determination of electron-affinity of Pd and Cu.

Figure 2.

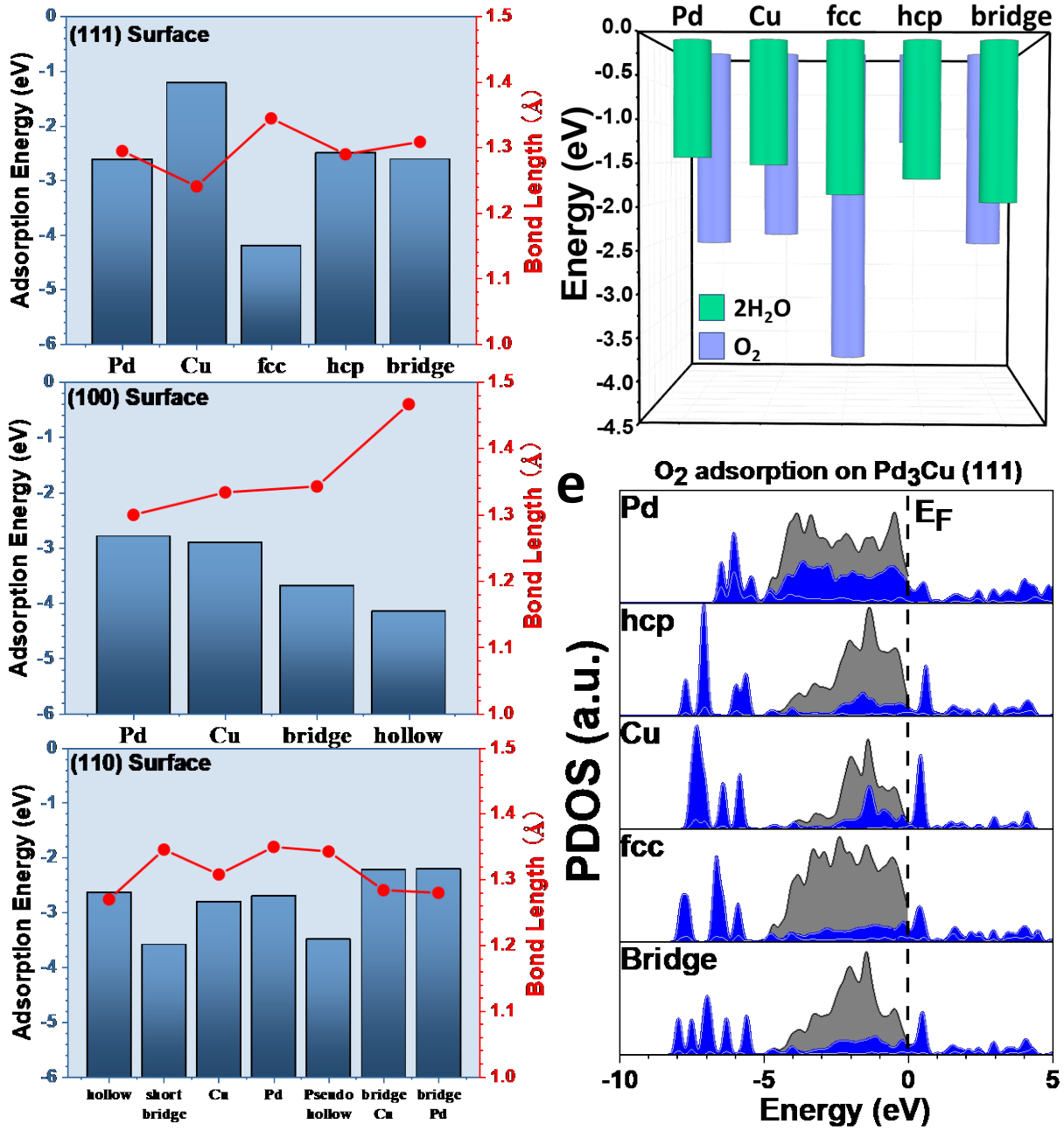

Figure 2 | The adsorption behaviours of O_2. (a)-(c) The adsorption energies and bond length of O_2 on active sites on (a) (111), (b)(110) and (c) (110) surfaces. (d) The adsorption energies of the initial reactant of alkaline ORR in (111) surfaces. (e) PDOS of the adsorption O_2 with surface metal. Blue = *sp* orbitals and Grey = *d* orbitals.

Figure 3.

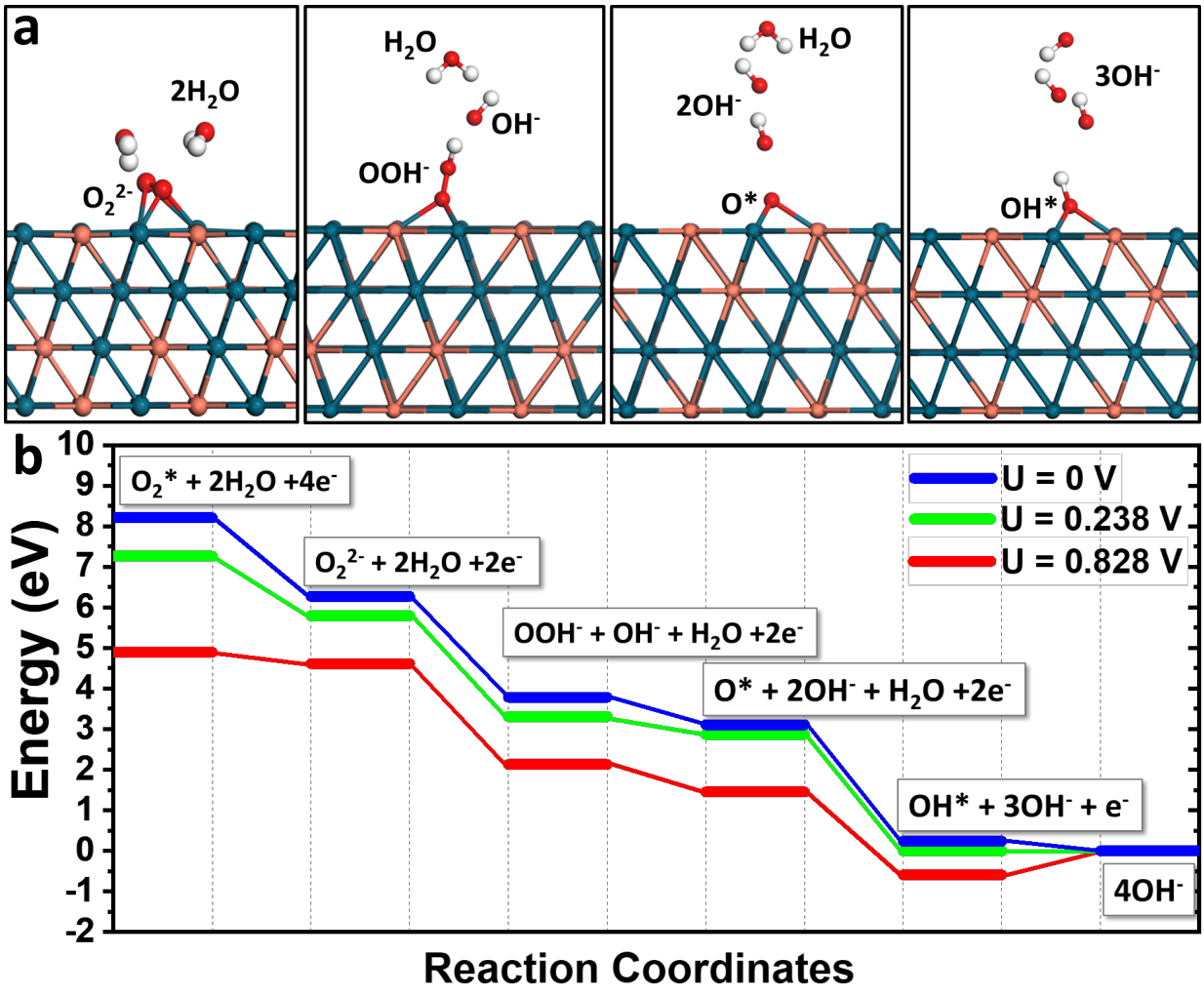

Figure 3 | (a) Optimized structure configurations of the reaction steps and (b) corresponding reaction energy path.

References

1. N. Markovic, T. Schmidt, V. Stamenkovi´c and P. Ross, ***Fuel cells***, 2001, 1, 105– 116.
2. K. B. Liew, W. R. W. Daud, M. Ghasemi, J. X. Leong, S. S. Lim and M. Ismail, ***International Journal of Hydrogen Energy***, 2014, 39, 4870–4883.
3. D. Banham, S. Ye, K. Pei, J.-i. Ozaki, T. Kishimoto and Y. Imashiro, ***Journal of Power Sources***, 2015, 285, 334–348.
4. F. Jaouen, E. Proietti, M. Lefèvre, R. Chenitz, J.-P. Dodelet, G. Wu, H. T. Chung, C. M. Johnston and P. Zelenay, Energy & Environmental ***Science***, 2011, 4, 114–130.
5. L. Dai, Y. Xue, L. Qu, H.-J. Choi and J.-B. Baek, Chemical reviews, 2015, 115, 4823–4892.
6. J. L. Fernández, V. Raghuveer, A. Manthiram and A. J. Bard, ***Journal of the American Chemical Society***, 2005, 127, 13100–13101.
7. H. Tang, J. Wang, H. Yin, H. Zhao, D. Wang, and Z. Tang, ***Advanced Materials***, 2015, 27, 1117-1123.
8. J. Sun, H. Yin, P. Liu, Y. Wang, X. Yao, Z. Tang and H. Zhao, ***Chemical Science***, 2016, 7, 5640-5646.
9. J. Sun, S. E. Lowe, L. Zhang, Y. Wang, K. Pang, Y. Wang, Y. Zhong, P. Liu, K. Zhao, Z. Tang, H. Zhao, ***Angew. Chem.*** 2018, 130, 16749.
10. J. Sun, D. Yang, S. Lowe, L. Zhang, Y. Wang, S. Zhao, P. Liu, Y. Wang, Z. Tang, H. Zhao, X. Yao, ***Advanced Energy Materials,*** 2018, 8, 1801495.
11. J. S. Spendelow and A. Wieckowski, ***Physical Chemistry Chemical Physics***, 2007,9, 2654–2675.
12. N. Ramaswamy and S. Mukerjee, ***Advances in Physical Chemistry***, 2012, 2012.
13. J. K. Nørskov, J. Rossmeisl, A. Logadottir, L. Lindqvist, J. R. Kitchin, T. Bligaard and H. Jonsson, ***The Journal of Physical Chemistry B***, 2004, 108, 17886–17892.
14. E. Antolini, Energy & Environmental Science, 2009, 2, 915–931.
15. O. Savadogo, K. Lee, K. Oishi, S. Mitsushima, N. Kamiya and K.-I. Ota, ***Electro-chemistry communications***, 2004, 6, 105–109 1388–2481.
16. J. Wu, S. Shan, J. Luo, P. Joseph, V. Petkov and C.-J. Zhong, ***ACS applied materials & interfaces***, 2015, 7, 25906–25913.
17. H. Zhang, Q. Hao, H. Geng and C. Xu, ***International Journal of Hydrogen Energy***, 2013, 38, 10029–10038.
18. J. Wu, S. Shan, J. Luo, P. Joseph, V. Petkov and C.-J. Zhong, ***ACS applied materials & interfaces***, 2015, 7, 25906–25913.
19. V. Stamenkovi´c, T. Schmidt, P. Ross and N. Markovi´c, ***Journal of Electroanalytical Chemistry***, 2003, 554, 191–199.
20. H. Yu, Y. Xue, B. Huang, L. Hui, C. Zhang, Y. Fang, Y. Liu, Y. Zhao, Y. Li, H. Liu, Y. Li, ***iScience***, 2019, 11, 31-41.
21. Y. Xue; B. Huang; Y. Yi; Y. Guo; Z. Zuo; Y. Li; Z. Jia; H. Liu; Y. Li, ***Nature Communications,*** 2018, 9 1460.
22. S. Mukerjee, S. Srinivasan, M. P. Soriaga and J. McBreen, ***Journal of the Electro-chemical Society***, 1995, 142, 1409–1422.
23. F. Fouda-Onana and O. Savadogo, Electrochimica Acta, 2009, 54, 1769–1776. 18 J. Greeley, J. K. Nørskov and M. Mavrikakis, ***Annual Review of Physical Chemistry***, 2002, 53, 319–348.
24. M. Shao, ***Journal of Power Sources***, 2011, 196, 2433–2444.

25. M. Wang, X. Qin, K. Jiang, Y. Dong, M. Shao and W.-B. Cai, ***The Journal of Physical Chemistry C***, 2017, 121, 3416–3423.
26. T. H. Yu, T. Hofmann, Y. Sha, B. V. Merinov, D. J. Myers, C. Heske and W. A. Goddard III, ***The Journal of Physical Chemistry C***, 2013, 117, 26598–26607.
27. V. R. Stamenkovic, B. S. Mun, K. J. Mayrhofer, P. N. Ross and N. M. Markovic, ***Journal of the American Chemical Society***, 2006, 128, 8813–8819.
28. J. Zhang, M. B. Vukmirovic, Y. Xu, M. Mavrikakis and R. R. Adzic, ***Angewandte Chemie International Edition***, 2005, 117, 2170–2173.
29. M. P. Hyman and J. W. Medlin, ***The Journal of Physical Chemistry C***, 2007, 111, 17052–17060.
30. T. McCrum and M. J. Janik, ***The Journal of Physical Chemistry C***, 2015, 120, 457–471.
31. Y. Qiu, L. Xin, Y. Li, I. T. McCrum, F. Guo, T. Ma, Y. Ren, Q. Liu, L. Zhou, S. Gu et al., ***Journal of the American Chemical Society***, 2018.